Assessment of aneuploidy concordance between clinical trophectoderm biopsy and blastocyst

Running Title:

Aneuploidy concordance within blastocysts

Authors:

Andrea R. Victor[1,2], Darren K. Griffin[2], Alan J. Brake[1], Jack C. Tyndall[1], Alex E. Murphy[1], Laura T. Lepkowsky[1], Archana Lal[1], Christo G. Zouves[1,3], Frank L. Barnes[1,3], Rajiv C. McCoy[4] and Manuel Viotti[1,3,*]

[1] Zouves Fertility Center, Foster City, California, USA;

[2] School of Biosciences, University of Kent, Canterbury, United Kingdom;

[3] Zouves Foundation for Reproductive Medicine, Foster City, California, USA.

[4] Department of Ecology and Evolutionary Biology, Princeton University, Princeton, New Jersey, USA.

*Corresponding author information: Manuel Viotti

manuel@zouvesfoundation.org

ABSTRACT

Study question:

Is a clinical trophectoderm (TE) biopsy a suitable predictor of chromosomal aneuploidy in blastocysts?

Summary answer:

In the analyzed group of blastocysts, a clinical TE biopsy was an excellent representative of blastocyst karyotype in cases of whole chromosome aneuploidy, but in cases of segmental (sub-chromosomal) aneuploidy, a TE biopsy was a poor representative of blastocyst karyotype.

What is known already:

Due to the phenomenon of chromosomal mosaicism, concern has been expressed about the possibility of discarding blastocysts classified as aneuploid by pre-implantation genetic testing for aneuploidy (PGT-A) that in fact contain a euploid Inner Cell Mass (ICM). Previously published studies investigating karyotype concordance between TE and ICM have examined small sample sizes and/or have utilized chromosomal analysis technologies superseded by Next Generation Sequencing (NGS). It is also known that blastocysts classified as mosaic by PGT-A can result in healthy births. TE re-biopsy of embryos classified

as aneuploid can potentially uncover new instances of mosaicism, but the frequency of such blastocysts is currently unknown.

Study design, size, duration:

45 patients donated 100 blastocysts classified as uniform aneuploids (non-mosaic) using PGT-A by NGS (n=93 whole chromosome aneuploids, n=7 segmental aneuploids). In addition to the original clinical TE biopsy used for PGT-A, each blastocyst was subjected to an ICM biopsy as well as a second TE biopsy. All biopsies were processed for chromosomal analysis by NGS, and karyotypes compared to the original TE biopsy.

Participants/materials, setting, methods:

Single IVF center with in-house PGT-A program and associated research laboratory.

Main results and the role of chance:

When one or more whole chromosomes were aneuploid in the clinical TE biopsy, the corresponding ICM was aneuploid in 90 out of 93 blastocysts (96.8%). When the clinical TE biopsy only contained segmental (sub-chromosomal) aneuploidies, the ICM was aneuploid in 4 out of 7 cases (57.1%). Blastocysts showing aneuploidy concordance between clinical TE biopsy and ICM were also aneuploid in a second TE biopsy in 86 out of 88 cases (97.7%). In blastocysts

displaying clinical TE-ICM discordance, a second TE biopsy was aneuploid in only 2 out of 6 cases (33.3%).

Limitations, reasons for caution:

All embryos in this study had an initial classification of 'aneuploid' and not 'euploid' or 'mosaic'. Therefore, the findings of this study refer specifically to a TE biopsy predicting aneuploidy in the remaining blastocyst, and cannot be extrapolated to deduce the ability of a TE biopsy to predict euploidy in the blastocyst. No conclusions should be drawn from this study about a mosaic TE biopsy's ability to predict the karyotype of the corresponding blastocyst. Caution should be exercised in generalizing the findings of the sample group of this study to the general IVF blastocyst population. The segmental aneuploidy group only contains 7 samples.

Wider implications of the findings:

The high rate of intra-blastocyst concordance observed in this study concerning whole chromosome aneuploidy contributes experimental evidence to the validation of PGT-A at the blastocyst stage. Concomitantly, the results suggest potential clinical value in reassessing blastocysts deemed aneuploid by TE re-biopsy in select cases, particularly in instances of segmental aneuploidies. This could impact infertility treatment for patients who only have blastocysts classified as aneuploid by PGT-A available.

Study funding/competing interest(s):

This study was supported by the Zouves Foundation for Reproductive Medicine and Zouves Fertility Center. The authors have no competing interest to disclose.

Trial registration number:

Not applicable

Keywords: Aneuploidy, Concordance, Blastocyst, PGT-A, Mosaic

INTRODUCTION

A number of clinical trials have reported improved IVF outcomes following the vetting of embryos for chromosomal abnormalities (Forman et al., 2013; Rubio et al., 2017; Scott et al., 2013; Yang et al., 2012), and yet the IVF community is still debating the appropriate use of preimplantation genetic testing for aneuploidy (PGT-A, previously called PGS) (Practice Committees of the American Society for Reproductive et al., 2018; Sermon et al., 2016). Skeptics of the technology condemn the assumption that a 5-10 cell biopsy is representative of the remaining embryo (Esfandiari et al., 2016; Gleicher and Orvieto, 2017). Indeed, the phenomenon of mosaicism, the condition of containing two or more cell lines with distinct chromosomal content (Taylor et al., 2014), provides a biological rationale for that concern. A karyotypic categorization of the trophectoderm (TE), the precursor to the placenta, might therefore not always be predictive of the inner cell mass (ICM), which gives rise to the fetus.

One of the potential consequences of misclassification of embryos during PGT-A is the deselection of viable embryos when a blastocyst is deemed aneuploid by TE biopsy but in fact contains a euploid ICM (Esfandiari et al., 2016; Schoolcraft et al., 2017; Vera-Rodriguez and Rubio, 2017). Some patients are only capable of producing embryos classified as aneuploid by PGT-A even after repeated IVF cycles, particularly with advanced age (Franasiak et al., 2014). Such cases invariably lead to the abandonment of infertility treatment.

Previous studies investigating rates of TE-ICM chromosomal concordance (expertly reviewed by Capalbo and Rienzi), while extremely valuable, have relied on limited sample sizes or methodologies that have recently been superseded by higher resolution genetic testing platforms (Capalbo and Rienzi, 2017). Next Generation Sequencing (NGS), has been heralded as a PGT-A technique with superior sensitivity for chromosomal mosaicism compared to aCGH, qPCR or SNP array (Fragouli et al., 2017; Harton et al., 2017; Maxwell et al., 2016; Munne et al., 2017; Munne and Wells, 2017) and has also been reported as highly effective in detecting segmental (i.e. sub-chromosomal) losses and gains with higher precision than previous methods (Lai et al., 2017).

The purpose of this study was specifically to test the hypothesis that a blastocyst embryo classified as aneuploid by NGS-based PGT-A correctly predicts the ploidy of the ICM in the majority of cases. Furthermore, by analyzing a second TE biopsy we determined the frequency of blastocysts originally classified as aneuploid that could be redefined as mosaic by re-biopsy.

MATERIALS AND METHODS

Embryos and clinical PGT-A analysis by NGS

Blastocysts derived from patients seeking infertility treatment were generated by in vitro fertilization and embryo culture as previously described (Victor et al., 2017), and were evaluated using the Gardner system (Gardner and Schoolcraft, 1999). As part of the embryo selection process, a clinical 5-10 cell TE biopsy was collected and blastocysts were vitrified. The clinical TE biopsies were subjected to whole genome amplification (WGA) with SurePlex reagents (Illumina) followed by NGS-based PGT-A using Illumina's VeriSeq kit (Illumina) on a MiSeq system (Illumina) according to the manufacturer's protocol and described in detail elsewhere (Vera-Rodriguez et al., 2016). For quality control, only samples satisfying the following cutoffs were used: number of Reads Passing Filter: >0.25M; Average Q-Score: >30; Alignment Score: >30; DLR (derivative log ratio): <0.4. Karyotype profiles were evaluated independently by three analysts and consensus determined. Copy number variation (CNV) for each chromosome was scored in Bluefuse Multi Analysis Software (Illumina) according to guidelines defined by the Preimplantation Genetic Diagnosis International Society (PGDIS), accessible at 'http://www.pgdis.org/docs/newsletter_071816.html': Profiles with copy number scale values <1.2 and >2.8 were recorded as aneuploid, those with values

between 1.8 and 2.2 were recorded as euploid, and all others were recorded as mosaic. These guidelines reflect the detection range of mosaicism by NGS PGT-A, validated in various cell- and DNA-mixing experiments (Fragouli et al., 2017; Maxwell et al., 2016; Munne et al., 2017; Munne and Wells, 2017). The resolution of VeriSeq NGS is validated to detect segmental (sub-chromosomal) aneuploidies of 20Mb or larger by the manufacturer, although detection of regions down to 1.81Mb have been reported using this platform (Zheng et al., 2015). In our center, we consider 'aneuploidy' to encompass both whole and segmental chromosome abnormalities.

Supernumerary blastocysts classified as 'aneuploid' (no mosaics) by PGT-A were donated to science by signed informed consent by 45 patients (average age of 36.5 ± 5.7) and de-identified. This study was approved by the institutional review board of the Zouves Foundation for Reproductive Medicine (OHRP IRB00011505).

ICM and Second TE Biopsy Collection and Analysis

ICM biopsies were isolated from vitrified-warmed blastocysts as outlined in the legend for Fig. 1A, basing the technique on a protocol described previously (Taylor et al., 2016) but omitting the exposure of samples to Ca^{2+}/Mg^{2+}-free medium. Immediately following ICM biopsy an additional TE biopsy was collected. All biopsies were washed three times to clear any loose cells or cellular

debris, and subsequently stored at -80°C until further processing. Biopsies were subjected to NGS-based PGT-A (as detailed above), and results evaluated independently by three analysts blinded to the analysis profile of the original, clinically reported TE biopsy.

For transparency, all karyotype profiles of every biopsy analyzed in this study are shown in the main or supplemental figures of the manuscript.

Immunofluorescence

Whole blastocysts or biopsies were immersed in fixation buffer containing 4% paraformaldehyde (EMS #15710) and 10% fetal bovine serum (FBS) (Seradigm 1500-050) in phosphate buffered saline (PBS) (Corning MT21040CM) for 10 minutes (min) at room temperature (rt), followed by three 1 min washes at rt in stain buffer, composed of 0.1% Triton X-100 (TX-100) (Sigma X100-100ML) and 10% FBS in PBS. Samples were then immersed in permeabilization buffer (0.5% TX-100, 10% FBS in PBS) for 30 min at rt, followed by three washes in stain buffer. Samples were then exposed to stain buffer containing both primary antibodies each in 1:200 concentrations over night at 4°C rocking on a nutator. Primary antibodies were mouse anti-human GATA3 (Thermo Fisher MA1-028) and rabbit anti-human OCT4A (Cell Signaling #2890). The next day, after three washes in stain buffer, samples were immersed in stain buffer containing both secondary antibodies each in 1:500 concentrations for 2-3 hours at rt. Secondary

antibodies were goat anti-mouse IgG AlexaFluor488 (Thermo Fisher A11029) and goat anti-rabbit IgG AlexaFluor647 (Thermo Fisher A21245). After three washes in stain buffer, samples were exposed to nuclear stain (Hoechst 33342, Thermo Fisher H3570) diluted at 1:1000 in stain buffer for 30 min at rt, followed by three more washes in stain buffer. Samples were placed in glass bottom dishes (MatTek P35G-1.5-20-C) in small drops of stain buffer overlaid with mineral oil (Sigma M5904), and imaged with a LSM 780 Confocal microscope (Zeiss).

Analysis of tissue relatedness

In cases of clinical TE-ICM karyotype discordance we confirmed tissue relatedness by a DNA fingerprinting method that utilizes SNP analysis and linkage disequilibrium known as 'Tilde' (Vohr et al., 2015). A full explanation of the adaptation of this method to PGT-A samples with low coverage NGS is detailed in Supplemental Data 1.

Statistical analysis of correlation between morphology and karyotype discordance

Analysis and graph preparation were performed in Prism 6 (GraphPad). Differences between groups were assessed by Chi-square test for trend with 95% confidence levels. Significance was defined when $P < 0.05$.

RESULTS

Isolation of ICM and Second TE Biopsies

We adopted a modified ICM-biopsy procedure previously outlined (Taylor et al., 2016), which permitted us to collect an ICM biopsy and subsequently a second TE biopsy in blastocysts (Fig. 1A and Video 1). Immunofluorescence was used to confirm accurate isolation of intended cells. In whole blastocysts the pluripotency factor OCT4 was present at high levels in the ICM and low levels in the TE, while GATA3 was exclusively expressed in cells of the TE as previously shown (Deglincerti et al., 2016). Analysis of matched TE-ICM biopsies from 12 blastocysts indicated that both biopsy types exclusively contained cells of their intended lineage and were devoid of contamination from the other cell type (Fig. 1B and Supplemental Fig. 1). Nuclear counterstain by Hoechst did not reveal any cells with fragmenting or apoptotic nuclear material, suggesting that the biopsy technique did not disrupt individual cells (Fig. 1B and Fig. S1). On average, TE biopsies comprised 7.6 cells (+/- 1.3 SD) while ICM biopsies comprised 7.3 cells (+/- 2.0 SD).

Clinical TE-ICM Biopsy Concordant Blastocysts

Of the 100 blastocysts originally classified as aneuploid by clinical (original) TE biopsy, 93 had ICMs that were also classified as aneuploid, which we denote as aneuploid-aneuploid concordant (Fig. 2 and Table I). Importantly,

when only considering blastocysts with whole chromosomal aneuploidies (single or multiple) in their clinical TE biopsies, aneuploidy in the ICM was present in 90 out of 93 cases (96.8%). On the other hand, when considering blastocysts with only segmental (sub-chromosomal) aneuploidies in their clinical TE biopsies, aneuploidy in the ICM was present in only 3 out of 7 cases (42.9%).

In aneuploid-aneuploid concordant blastocysts, analysis of second TE biopsies showed aneuploidy in 86 out of 88 cases, equaling 97.7% (Table I). The remaining two samples showed a mosaic pattern in their respective second TE biopsies. In five samples a second TE biopsy could not be retrieved.

The 93 clinical TE-ICM aneuploid-aneuploid concordant blastocysts could be further subdivided in two groups. 79 were blastocysts that had perfectly matching karyotypes in the clinical TE and ICM biopsies (i.e., all the same chromosomes possessed the same aneuploidies in both tissues), which we denoted as aneuploid-aneuploid *perfect* concordant (Fig. 2, Table I, and for the karyotypic profiles see Supplemental Fig. 2). Such instances are likely consequences of meiotic errors, as the identical aneuploidy is present in both TE and ICM tissues (see Supplemental Data 2 for more detailed interpretations).

The remaining 14 out of 93 blastocysts had dissimilar aneuploidies in the clinical TE and ICM biopsies, which we denoted as aneuploid-aneuploid *imperfect* concordant (Fig. 2, Table I, and for the karyotypic profiles see Supplemental Fig. 2). Interestingly, most such blastocysts (10 out of 14) showed the same aneuploid chromosome(s) in the ICM biopsy as the clinical TE biopsy

(presumed consequence of meiotic error), but contained additional mosaic events in the ICM (resulting from mitotic error), often segmental in nature.

See Supplemental Data 2 for interpretations of chromosomal error etiologies in samples of the aneuploid-aneuploid *imperfect* concordant group.

Clinical TE-ICM Biopsy Discordant Blastocysts

Of the 100 blastocysts tested, we observed two cases in which the clinical TE biopsy was uniformly aneuploid but the ICM was mosaic (Fig. 2, Table I, and for the karyotypic profiles see Fig. 3) Supplemental Data 2 contains more detailed interpretations of their karyotypes.

Five out of 100 blastocysts had euploid ICMs while their clinical TE biopsies contained aneuploidies (Fig. 2, Table I, and for the karyotypic profiles see Fig. 3). Blastocyst #96 was the only case in which the clinical TE biopsy had a whole chromosomal aneuploidy (gain of chromosome 12, note that the karyotype profile enters into the 2.8-3.0 copy number region) but displayed euploidy in the ICM as well as in the second TE biopsy.

The remaining four samples (blastocysts #97-#100) contained segmental aneuploidies in their original TE biopsies, but euploid ICM biopsies. For blastocyst #97, the clinical and second TE biopsies contained the same segmental aneuploidy, thereby suggesting euploidy confined to the ICM. This would be consistent with a mitotic event happening before or at the time of lineage segregation but in the progenitor cell of a large part of the TE. Blastocysts #98 and #99 displayed mosaicism in their respective second TE

biopsies, revealing the occurrence of mitotic errors in the TE lineage. For one blastocyst (#100), the second TE biopsy did not yield results due to a failed WGA reaction. (Global WGA failure rate for this study is 1 out of 221, or 0.4%). In total, of the clinical TE-ICM discordant blastocysts (aneuploid-euploid or aneuploid-mosaic) yielding information in the second TE biopsy, only 2 out of 6 (33.3%) were uniformly aneuploid.

In cases of clinical TE-ICM biopsy discordance, there existed the possibility of sample contamination or mislabeling. Notably, in the 100 embryos tested, the sex chromosomes (XX or XY) were always concordant between biopsies taken within the same blastocyst. Further, for each of the seven blastocysts that produced discordant results, we performed DNA fingerprinting to confirm that the clinical TE and ICM biopsies were derived from the same respective embryos (Fig. 4 and Supplemental Fig. 3).

Finally, we determined whether poor blastocyst morphology impacted karyotype discordance. The analysis indicated that neither blastocyst stage nor ICM/TE grade affected the likelihood of intra-blastocyst karyotype inconsistencies (Supplemental Fig. 4).

DISCUSSION

Some parties have argued that PGT-A should not be performed under any circumstance and one of the criticisms of the technology questions whether a clinical TE biopsy is a valid genetic representative of the embryo (Esfandiari et al., 2016; Mastenbroek and Repping, 2014; Sermon et al., 2016). A study basing its rationale on mathematical modeling has claimed that a typical TE cell biopsy cannot determine embryo ploidy accurately enough for clinical use (Gleicher et al., 2017). One of the ensuing concerns that has been expressed is the possibility of erroneously discarding viable embryos (Practice Committees of the American Society for Reproductive et al., 2018). Here however, we provide experimental evidence using NGS that a TE biopsy classified as aneuploid is commonly predictive of aneuploidy in the ICM. In our experience, a whole chromosome aneuploidy in a clinical TE biopsy is predictive of aneuploidy in the ICM in 96.8% of cases (sample size n=93), although for a segmental aneuploidy this decreases significantly to 42.9% (n=7).

A blastocyst with an aneuploid TE and ICM due to meiotic error is in principle exceptionally unlikely to result in healthy pregnancy (Adashi and McCoy, 2017). Although various corrective mechanisms for aneuploidies in human embryos have been proposed (differential proliferation/depletion, preferential lineage allocation, self-correction) (Capalbo and Rienzi, 2017; McCoy, 2017) and have also been conceptually demonstrated in mouse embryos (Bolton et al., 2016) and human embryonic stem cells (hESC) (Munne et al.,

2005), most models describe the out-competition of aneuploid cells by euploid cells in the mosaic setting, not the conversion of an entirely aneuploid embryo to an entirely euploid one.

The observation that segmentals had a drastically different rate of clinical TE-ICM discordance compared to whole chromosome aneuploids highlights the difference in mechanistic origins of these two types of aneuploidies. Whole chromosome aneuploidies can arise during meiosis or mitosis by different mechanisms that include non-disjunction, anaphase lag, and endoreplication (Taylor et al., 2014), but the majority are believed to be derived from meiotic errors in the oocyte (Nagaoka et al., 2012). The majority of segmental aneuploidies on the other hand are mitotic in origin and are thought to arise during the first few cell divisions after fertilization (Babariya et al., 2017). Cell cycle control is thought to be more lax during the first days of embryogenesis due to rapid mitoses primarily controlled by maternal RNA and proteins, leading to an increased incidence of double strand breaks which upon faulty correction mechanisms result in segmental duplications or deletions when left unresolved by a strained cell cycle machinery (Babariya et al., 2017). Consequently, segmental aneuploidies will often be represented in mosaic configurations at a whole blastocyst level, likely translating in the high TE-ICM discordance rate observed for the segmental aneuploidy group in this study.

Out of 93 blastocysts with whole chromosome aneuploidies (single or multiple) in a clinical TE biopsy, three embryos had a discordant ICM: two contained mosaic ICM biopsies, and one had a euploid ICM. Consequently, the

366 karyotype of these three blastocysts should be re-classified from aneuploid to
367 mosaic, since on a whole embryo level they contained aneuploid and euploid
368 cells. This re-categorization would have changed the status of the blastocysts
369 from ‘not recommended for transfer’ to ‘possible transfer if no euploid embryos
370 available’. Mosaic embryos have recently been considered for transfer in several
371 clinics, producing healthy pregnancies albeit with considerably lower implantation
372 rates than blastocysts classified as euploid (Fragouli et al., 2017; Lledo et al.,
373 2017; Munne et al., 2017; Spinella et al., 2018).

374 From a clinical standpoint, our findings may support re-biopsy of
375 blastocysts in patients that have only produced embryos classified as aneuploid
376 (particularly segmentals) by initial TE biopsy after repeated IVF cycles, an
377 occurrence that happens with relative frequency especially with advanced
378 maternal age (Franasiak et al., 2014). It could also affect those patients that have
379 unsuccessfully transferred their embryos classified as ‘euploid’ and ‘mosaic’, and
380 only have ‘aneuploid’ samples remaining. In our study, all blastocysts had an
381 initial, clinical TE biopsy that was uniformly aneuploid. When a second TE biopsy
382 was either mosaic or euploid, such a blastocyst had a 66% chance to contain an
383 ICM that was either mosaic or euploid as well. On the other hand, in cases where
384 the second TE biopsy was aneuploid, the ICM was mosaic in only 1.1% of cases,
385 and there were no euploid ICM instances. Therefore, our results suggest that TE
386 re-biopsy can reveal whether the ICM is mosaic or euploid, helping to identify
387 new blastocysts for possible clinical use that were originally not recommended
388 for transfer due to aneuploidy in the clinical TE biopsy. Importantly, while the act

of re-biopsy might negatively affect blastocysts, re-biopsied blastocysts can lead to healthy pregnancies albeit with lower efficiency than single-biopsied blastocysts (Bradley et al., 2017). Nevertheless, more research is necessary to determine the short and long term effects of TE re-biopsy, and recommendation of routine re-biopsy of blastocysts classified as aneuploid is undoubtedly premature.

The confirmed existence of clinical TE-ICM discordant embryos could also help explain the rare accounts of healthy pregnancies resulting from transfer of embryos classified as aneuploid by PGT-A (Gleicher et al., 2016), although it must be pointed out that to our knowledge, there exist no reports of such events when using blastocyst stage NGS-based PGT-A.

It is important to note that our determined rates of clinical TE-ICM concordance apply specifically to blastocysts classified as ‘uniform aneuploid’ (no mosaics) by PGT-A. Having observed an overall 7% clinical TE-ICM discordance rate in our samples, we cannot assume the inverse: that 7% of blastocysts classified as euploid contain an aneuploid ICM. A further intriguing and clinically important question is what a clinical TE biopsy showing mosaicism says about the ICM. Unfortunately, our study cannot shed light on that point.

A further limitation of this study was that not all cells were analyzed for intra-blastocyst karyotypic concordance. The ICM biopsies isolated (averaging 7.3 cells) collected the bulk of ICM cells but invariably left residual ICM cells behind. On average, we collected 15 TE cells from the two combined TE biopsies of each blastocyst, hence a substantial portion of the TE was left unanalyzed.

From the technical standpoint we were unable to isolate more cells from a specific tissue without contamination from the other lineage. As a result, instances of karyotype discordance could remain concealed.

While highly controversial, the concept of transferring embryos testing aneuploid by PGT-A is a real subject of discussion in both scientific (Gleicher et al., 2016) and mainstream media (Hall, 2017). The upheaval created by these viewpoints has partly been bolstered by the yet unspecified capability of a single clinical TE biopsy to reflect the state of the ICM and remaining TE. With regard to this question our findings contribute experimental validation on the practice of PGT-A at the blastocyst stage, considering the high intra-blastocyst aneuploidy concordance rates, especially in the case of whole chromosome losses or gains. If indeed the group of blastocysts analyzed in this study is representative of the general body of IVF blastocysts, it would mean that when selecting an embryo classified as ‘aneuploid’ by PGT-A for uterine transfer, it almost always contains aneuploidy in the entire blastocyst. Unless robust self-correction mechanisms do in fact exist, said embryo would invariable lead to failed implantation, miscarriage, or chromosomally abnormal babies. Segmental aneuploidies on the other hand are rarely concordant; if our observations are confirmed in a larger sample group they should be regarded as their own distinct class when prioritizing or de-selecting embryos for transfer in the clinic.

435 **Authors' Roles**

436 A.R.V., D.K.G., A.L., C.G.Z., F.L.B., R.C.M., and M.V. designed the experiments.

437 A.R.V, A.J.B., J.C.T. A.E.M., L.T.L. R.C.M., and M.V. performed the experiments.

438 A.R.V., D.K.G., F.L.B., and M.V. wrote the manuscript.

439 A.J.B., J.C.T. A.E.M., L.T.L., A.L., C.G.Z., and R.C.M edited the manuscript.

440

441 **Acknowledgements**

442 We would like to thank the entire ZFC staff for supporting this study in many

443 ways, including sample storage, reagent preparation, and discussions.

444

445 **Funding**

446 This study was supported by the Zouves Foundation for Reproductive Medicine

447 and Zouves Fertility Center.

448

449 **Conflict of Interest**

450 The authors have no conflict of interest to declare.

FIGURE LEGENDS

Figure 1.

Validation of biopsy and PGT-A methods used in the study

(A) Stills from video depicting isolation of ICM biopsy in blastocysts. The blastocyst is immobilized with a holding pipet touching the polar TE (adjacent to the ICM), and laser pulses are administered through the zona and mural TE opposite the ICM creating an opening. A biopsy pipette is introduced and guided to the ICM, which is suctioned out through the opening. Once a portion of ICM cells are extracted past the zona, they are exposed to laser pulses aimed at cell-cell junctions to isolate a 5-10 cell biopsy.

(B) Nuclear counterstain (Hoechst) and immunofluorescent stains for the TE marker GATA3 and ICM marker OCT4 in a whole human blastocyst and isolated TE and ICM biopsies. See additional samples in Figure S1. Scale bars = 25μm.

Figure 2.

Summary of paired clinical TE-ICM comparison results

Dot plot displays results for all blastocysts, regardless of aneuploidy type. Pie charts depict data stratified by nature of aneuploidy detected in the original TE biopsy for each blastocyst.

Figure 3.

NGS-based PGT-A karyotype profiles for biopsies in blastocysts with discordant clinical TE-ICM patterns

See Table I for the interpretation of each profile.

Figure 4.

Log-likelihood ratios of relatedness between tissues in blastocysts with clinical TE-ICM discordance

In green, controls comparing biopsies from embryos derived from patients expected to be unrelated, showing negative values. In red, comparisons between biopsies from blastocysts derived from the same patient (full-sibs) showing positive values. In purple, comparisons between clinical TE

and ICM biopsies for each blastocyst classified as discordant in the study, showing highly positive log-likelihood ratios of relatedness.

Supplemental Figure 1.

Validation of contamination-free ICM and TE biopsy technique

Nuclear counterstain (Hoechst) and immunofluorescent stains for the TE marker GATA3 and ICM marker OCT4 in matched isolated TE and ICM biopsies. Numbers in nuclear stain panels indicate total number of cells for each biopsy. Numbers in TE stain panels indicate incidence of cells positive for GATA3. Numbers in ICM stain panels indicate incidence of cells with high nuclear signal for OCT4. Scale bars = 25μm.

Supplemental Figure 2.

Karyotype profiles analyzed in this study (continued from Fig. 3)

Use Table I as a reference for resulting analysis.

Supplemental Figure 3.

Genotypes of discordant blastocysts visualized in reference ancestry space

Supplemental Figure 4

Analysis of correlation between morphology and intra-blastocyst karyotype discordance

Blastocysts were evaluated using the Gardner system, that assigns a number score for blastocyst expansion stage (1-6 from least to most progressed), and letter scores for ICM and TE grades (C-A from worst to best quality) (Gardner and Schoolcraft, 1999). Stage of blastocyst was analyzed when there was any intra-blastocyst karyotype inconsistency (A), when an inconsistency was specific to the ICM (B), and when an inconsistency was specific to the TE (C). Grade of the ICM was analyzed when there was any karyotype inconsistency between clinical TE biopsy and the ICM (D). Grade of the TE was analyzed when there was any karyotype inconsistency between clinical TE and second TE biopsy (E). Note that in graphs A, C, and D, sample numbers do not add up to 100 because in six cases the second TE biopsy was not processed (in five cases the biopsy could not be collected, and in one case there was a failed WGA reaction.

TABLE LEGENDS

Table I. List of blastocysts, clinical TE, ICM, and second TE biopsies analyzed in this study.

Supplemental Table I. Blastocysts and assigned 1000 Genomes super-populations.

Supplemental Data 1. Adaptation of 'Tilde' to PGT-A samples with low coverage NGS.

Supplemental Data 2. Additional interpretations of chromosomal error etiologies in blastocysts.

BIBLIOGRAPHY

Adashi, E.Y., and McCoy, R.C. (2017). Technology versus biology: the limits of pre-implantation genetic screening: Better methods to detect the origin of aneuploidy in pre-implantation embryos could improve the success rate of artificial reproduction. EMBO Rep *18*, 670-672.

Babariya, D., Fragouli, E., Alfarawati, S., Spath, K., and Wells, D. (2017). The incidence and origin of segmental aneuploidy in human oocytes and preimplantation embryos. Hum Reprod *32*, 2549-2560.

Bolton, H., Graham, S.J., Van der Aa, N., Kumar, P., Theunis, K., Fernandez Gallardo, E., Voet, T., and Zernicka-Goetz, M. (2016). Mouse model of chromosome mosaicism reveals lineage-specific depletion of aneuploid cells and normal developmental potential. Nat Commun *7*, 11165.

Bradley, C.K., Livingstone, M., Traversa, M.V., and McArthur, S.J. (2017). Impact of multiple blastocyst biopsy and vitrification-warming procedures on pregnancy outcomes. Fertil Steril *108*, 999-1006.

Capalbo, A., and Rienzi, L. (2017). Mosaicism between trophectoderm and inner cell mass. Fertil Steril *107*, 1098-1106.

Deglincerti, A., Croft, G.F., Pietila, L.N., Zernicka-Goetz, M., Siggia, E.D., and Brivanlou, A.H. (2016). Self-organization of the in vitro attached human embryo. Nature *533*, 251-254.

Esfandiari, N., Bunnell, M.E., and Casper, R.F. (2016). Human embryo mosaicism: did we drop the ball on chromosomal testing? J Assist Reprod Genet *33*, 1439-1444.

579 Forman, E.J., Hong, K.H., Ferry, K.M., Tao, X., Taylor, D., Levy, B., Treff, N.R.,
580 and Scott, R.T., Jr. (2013). In vitro fertilization with single euploid blastocyst
581 transfer: a randomized controlled trial. Fertil Steril *100*, 100-107 e101.

582 Fragouli, E., Alfarawati, S., Spath, K., Babariya, D., Tarozzi, N., Borini, A., and
583 Wells, D. (2017). Analysis of implantation and ongoing pregnancy rates following
584 the transfer of mosaic diploid-aneuploid blastocysts. Hum Genet *136*, 805-819.

585 Franasiak, J.M., Forman, E.J., Hong, K.H., Werner, M.D., Upham, K.M., Treff,
586 N.R., and Scott, R.T., Jr. (2014). The nature of aneuploidy with increasing age of
587 the female partner: a review of 15,169 consecutive trophectoderm biopsies
588 evaluated with comprehensive chromosomal screening. Fertil Steril *101*, 656-663
589 e651.

590 Gardner, D.K., and Schoolcraft, W.B. (1999). In vitro culture of human
591 blastocysts. . In Towards reproductive certainty: fertility and genetics beyond, J.
592 R., and M. D., eds. (Camforth, UK: Parthenon Publishing), pp. 378-388.

593 Gleicher, N., Metzger, J., Croft, G., Kushnir, V.A., Albertini, D.F., and Barad, D.H.
594 (2017). A single trophectoderm biopsy at blastocyst stage is mathematically
595 unable to determine embryo ploidy accurately enough for clinical use. Reprod
596 Biol Endocrinol *15*, 33.

597 Gleicher, N., and Orvieto, R. (2017). Is the hypothesis of preimplantation genetic
598 screening (PGS) still supportable? A review. J Ovarian Res *10*, 21.

599 Gleicher, N., Vidali, A., Braverman, J., Kushnir, V.A., Barad, D.H., Hudson, C.,
600 Wu, Y.G., Wang, Q., Zhang, L., Albertini, D.F*., et al.* (2016). Accuracy of
601 preimplantation genetic screening (PGS) is compromised by degree of
602 mosaicism of human embryos. Reprod Biol Endocrinol *14*, 54.

603 Hall, S.S. (2017). A new last chance. In New York Magazine.

Harton, G.L., Cinnioglu, C., and Fiorentino, F. (2017). Current experience concerning mosaic embryos diagnosed during preimplantation genetic screening. Fertil Steril *107*, 1113-1119.

Lai, H.H., Chuang, T.H., Wong, L.K., Lee, M.J., Hsieh, C.L., Wang, H.L., and Chen, S.U. (2017). Identification of mosaic and segmental aneuploidies by next-generation sequencing in preimplantation genetic screening can improve clinical outcomes compared to array-comparative genomic hybridization. Mol Cytogenet *10*, 14.

Lledo, B., Morales, R., Ortiz, J.A., Blanca, H., Ten, J., Llacer, J., and Bernabeu, R. (2017). Implantation potential of mosaic embryos. Syst Biol Reprod Med *63*, 206-208.

Mastenbroek, S., and Repping, S. (2014). Preimplantation genetic screening: back to the future. Hum Reprod *29*, 1846-1850.

Maxwell, S.M., Colls, P., Hodes-Wertz, B., McCulloh, D.H., McCaffrey, C., Wells, D., Munne, S., and Grifo, J.A. (2016). Why do euploid embryos miscarry? A case-control study comparing the rate of aneuploidy within presumed euploid embryos that resulted in miscarriage or live birth using next-generation sequencing. Fertil Steril *106*, 1414-1419 e1415.

McCoy, R.C. (2017). Mosaicism in Preimplantation Human Embryos: When Chromosomal Abnormalities Are the Norm. Trends Genet *33*, 448-463.

Munne, S., Blazek, J., Large, M., Martinez-Ortiz, P.A., Nisson, H., Liu, E., Tarozzi, N., Borini, A., Becker, A., Zhang, J.*, et al.* (2017). Detailed investigation into the cytogenetic constitution and pregnancy outcome of replacing mosaic blastocysts detected with the use of high-resolution next-generation sequencing. Fertil Steril *108*, 62-71 e68.

629 Munne, S., Velilla, E., Colls, P., Garcia Bermudez, M., Vemuri, M.C., Steuerwald,
630 N., Garrisi, J., and Cohen, J. (2005). Self-correction of chromosomally abnormal
631 embryos in culture and implications for stem cell production. Fertil Steril *84*,
632 1328-1334.

633 Munne, S., and Wells, D. (2017). Detection of mosaicism at blastocyst stage with
634 the use of high-resolution next-generation sequencing. Fertil Steril *107*, 1085-
635 1091.

636 Nagaoka, S.I., Hassold, T.J., and Hunt, P.A. (2012). Human aneuploidy:
637 mechanisms and new insights into an age-old problem. Nat Rev Genet *13*, 493-
638 504.

639 Practice Committees of the American Society for Reproductive, M., the Society
640 for Assisted Reproductive Technology. Electronic address, A.a.o., Practice
641 Committees of the American Society for Reproductive, M., and the Society for
642 Assisted Reproductive, T. (2018). The use of preimplantation genetic testing for
643 aneuploidy (PGT-A): a committee opinion. Fertil Steril *109*, 429-436.

644 Rubio, C., Bellver, J., Rodrigo, L., Castillon, G., Guillen, A., Vidal, C., Giles, J.,
645 Ferrando, M., Cabanillas, S., Remohi, J.*, et al.* (2017). In vitro fertilization with
646 preimplantation genetic diagnosis for aneuploidies in advanced maternal age: a
647 randomized, controlled study. Fertil Steril *107*, 1122-1129.

648 Schoolcraft, W., Meseguer, M., and Global Fertility Alliance. Electronic address,
649 a.t.i.c. (2017). Paving the way for a gold standard of care for infertility treatment:
650 improving outcomes through standardization of laboratory procedures. Reprod
651 Biomed Online *35*, 391-399.

652 Scott, R.T., Jr., Upham, K.M., Forman, E.J., Hong, K.H., Scott, K.L., Taylor, D.,
653 Tao, X., and Treff, N.R. (2013). Blastocyst biopsy with comprehensive
654 chromosome screening and fresh embryo transfer significantly increases in vitro

655 fertilization implantation and delivery rates: a randomized controlled trial. Fertil
656 Steril *100*, 697-703.

657 Sermon, K., Capalbo, A., Cohen, J., Coonen, E., De Rycke, M., De Vos, A.,
658 Delhanty, J., Fiorentino, F., Gleicher, N., Griesinger, G.*, et al.* (2016). The why,
659 the how and the when of PGS 2.0: current practices and expert opinions of
660 fertility specialists, molecular biologists, and embryologists. Mol Hum Reprod *22*,
661 845-857.

662 Spinella, F., Fiorentino, F., Biricik, A., Bono, S., Ruberti, A., Cotroneo, E., Baldi,
663 M., Cursio, E., Minasi, M.G., and Greco, E. (2018). Extent of chromosomal
664 mosaicism influences the clinical outcome of in vitro fertilization treatments. Fertil
665 Steril *109*, 77-83.

666 Taylor, T.H., Gitlin, S.A., Patrick, J.L., Crain, J.L., Wilson, J.M., and Griffin, D.K.
667 (2014). The origin, mechanisms, incidence and clinical consequences of
668 chromosomal mosaicism in humans. Hum Reprod Update *20*, 571-581.

669 Taylor, T.H., Griffin, D.K., Katz, S.L., Crain, J.L., Johnson, L., and Gitlin, S.
670 (2016). Technique to 'Map' Chromosomal Mosaicism at the Blastocyst Stage.
671 Cytogenet Genome Res *149*, 262-266.

672 Vera-Rodriguez, M., Michel, C.E., Mercader, A., Bladon, A.J., Rodrigo, L.,
673 Kokocinski, F., Mateu, E., Al-Asmar, N., Blesa, D., Simon, C.*, et al.* (2016).
674 Distribution patterns of segmental aneuploidies in human blastocysts identified
675 by next-generation sequencing. Fertil Steril *105*, 1047-1055 e1042.

676 Vera-Rodriguez, M., and Rubio, C. (2017). Assessing the true incidence of
677 mosaicism in preimplantation embryos. Fertil Steril *107*, 1107-1112.

678 Victor, A.R., Brake, A.J., Tyndall, J.C., Griffin, D.K., Zouves, C.G., Barnes, F.L.,
679 and Viotti, M. (2017). Accurate quantitation of mitochondrial DNA reveals uniform

levels in human blastocysts irrespective of ploidy, age, or implantation potential. Fertil Steril *107*, 34-42 e33.

Vohr, S.H., Buen Abad Najar, C.F., Shapiro, B., and Green, R.E. (2015). A method for positive forensic identification of samples from extremely low-coverage sequence data. BMC Genomics *16*, 1034.

Yang, Z., Liu, J., Collins, G.S., Salem, S.A., Liu, X., Lyle, S.S., Peck, A.C., Sills, E.S., and Salem, R.D. (2012). Selection of single blastocysts for fresh transfer via standard morphology assessment alone and with array CGH for good prognosis IVF patients: results from a randomized pilot study. Mol Cytogenet *5*, 24.

Zheng, H., Jin, H., Liu, L., Liu, J., and Wang, W.H. (2015). Application of next-generation sequencing for 24-chromosome aneuploidy screening of human preimplantation embryos. Mol Cytogenet *8*, 38.

TABLE I

Clinical TE-ICM Aneuploid-Aneuploid Perfect Concordant

Blastocyst Study id#	Gardner Grade	Clinical TE Biopsy	ICM Biopsy	Second TE Biopsy
1	4BB	45,XY,-4	45,XY,-4	45,XY,-4
2	4BB	45,XX,-7	45,XX,-7	45,XX,-7
3	5BB	45,XX,-8	45,XX,-8	46,XX,-8*,+15*,+20*
4	3AB	45,XY,-8	45,XY,-8	45,XY,-8
5	5BC	45,XX,-10	45,XX,-10	45,XX,-10
6	4BB	45,XY,-11	45,XY,-11	45,XY,-11
7	5BB	45,XX,-13	45,XX,-13	45,XX,-13
8	5BC	45,XY,-13	45,XY,-13	n/a
9	5BC	45,XY,-14	45,XY,-14	45,XY,-14
10	4BB	45,XY,-14	45,XY,-14	45,XY,-14
11	2BB	45,XX,-15	45,XX,-15	45,XX,-15
12	4BC	45,XX,-15	45,XX,-15	n/a
13	3BB	45,XX,-16	45,XX,-16	45,XX,-16
14	4BC	45,XX,-16	45,XX,-16	45,XX,-16
15	4BB	45,XX,-16	45,XX,-16	45,XX,-16
16	4BB	45,XY,-16	45,XY,-16	45,XY,-16
17	5CC	45,XY,-16	45,XY,-16	45,XY,-16
18	5CC	45,XX,-17	45,XX,-17	45,XX,-17
19	5AB	45,XY,-18	45,XY,-18	45,XY,-18,del(10)(q11.21q26.3)*
20	4BB	45,XX,-21	45,XX,-21	45,XX,-21
21	5BB	45,XX,-21	45,XX,-21	45,XX,-21
22	4CB	45,XY,-21	45,XY,-21	45,XY,-21
23	5BB	45,XX,-22	45,XX,-22	45,XX,-22
24	4BB	45,XX,-22	45,XX,-22	45,XX,-22
25	5BB	45,XY,-22	45,XY,-22	45,XY,-22
26	4BB	45,XY,-22	45,XY,-22	45,XY,+4*,-22
27	4AA	45,XY,-22	45,XY,-22	45,XY,-22
28	4BB	45,X	45,X	46,XX,dup(X)(p22.33p21.1),dup(X)(q22.3q25)*
29	5BC	47,XX,+1	47,XX,+1	47,XX,+1
30	4BC	47,XY,+4	47,XY,+4	47,XY,+4
31	4AB	47,XX,+13	47,XX,+13	47,XX,+13
32	3BB	47,XX,+13	47,XX,+13	47,XX,+13
33	5AA	47,XY,+15	47,XY,+15	47,XY,+15
34	4CB	47,XX,+16	47,XX,+16	47,XX,+16
35	3AB	47,XX,+16	47,XX,+16	47,XX,+16
36	5BB	47,XX,+16	47,XX,+16	n/a
37	5BB	47,XY,+16	47,XY,+16	47,XY,+16
38	4BB	47,XY,+16	47,XY,+16	47,XY,+16
39	4BC	47,XY,+16	47,XY,+16	47,XY,+16
40	5BB	47,XY,+17	47,XY,+17	47,XY,-10*,+17
41	4BB	47,XY,+18	47,XY,+18	47,XY,+18
42	4CB	47,XY,+18	47,XY,+18	47,XY,+18
43	5BB	47,XY,+19	47,XY,+19	47,XY,+19
44	5AB	47,XX,+20	47,XX,+20	47,XX,+20
45	4BC	47,XX,+21	47,XX,+21	47,XX,+21
46	5CB	48,XX,+21(x2)	48,XX,+21(x2)	48,XX,+21(x2)
47	4BB	47,XX,+22	47,XX,+22	47,XX,+22
48	4AA	47,XX,+22	47,XX,+22	47,XX,+22
49	5AB	47,XX,+22	47,XX,+22	47,XX,+22
50	4BB	47,XY,+22	47,XY,+22	47,XY,+22
51	5CC	47,XY,+22	47,XY,+22	47,XY,+22
52	4BC	47,XY,+22	47,XY,+22	47,XY,+22
53	3CC	47,XY,+22	47,XY,+22	47,XY,+22,del(1)(q25.2q44)
54	3BB	44,XY,-10,-22	44,XY,-10,-22	44,XY,-10,-22
55	4BB	46,XX,-12,+16	46,XX,-12,+16	46,XX,-12,+16
56	4CC	44,XX,-14,-19	44,XX,-14,-19	44,XX,-14,-19
57	4BB	44,XY,-18,-21	44,XY,-18,-21	44,XY,-18,-21
58	4BC	46,XY,-19,+22	46,XY,-19,+22	n/a
59	5BB	46,XY,-21,+22	46,XY,-21,+22	46,XY,-21,+22
60	5CB	48,XY,+2,+3	48,XY,+2,+3	48,XY,+2,+3
61	4BB	46,XY,+3,-22	46,XY,+3,-22	n/a
62	4AA	48,XX,+5,+9	48,XX,+5,+9	48,XX,+5,+9
63	4AC	46,XX,+6,-15	46,XX,+6,-15	46,XX,+6,-15
64	5BB	48,XY,+8,+16	48,XY,+8,+16	48,XY,+8,+16,del(2)(q21.1q37.3)*
65	3BB	48,XX,+9,+16	48,XX,+9,+16	48,XX,+9,+16
66	3BB	48,XX,+9,+22	48,XX,+9,+22	48,XX,+9,+22
67	4BB	48,XX,+10,+18	48,XX,+10,+18	48,XX,+10,+18
68	5AB	48,XY,+16,+21	48,XY,+16,+21	48,XY,+16,+21
69	5BB	46,XX,+18,-22	46,XX,+18,-22	46,XX,+18,-22
70	3BA	45,XX,-11,+12,-21	45,XX,-11,+12,-21	45,XX,-11,+12,-21
71	4CB	47,XY,+1,-13,+21	47,XY,+1,-13,+21	47,XY,+1,-13,+21
72	3BB	47,XY,+11,+18,-20	47,XY,+11,+18,-20	47,XY,+11,+18,-20
73	5BC	47,XY,+14,-15,+19	47,XY,+14,-15,+19	47,XY,+14,-15,+19
74	5BC	49,XX,+16,+18,+19	49,XX,+16,+18,+19	48,XX,+16,+18,+19*
75	4AB	48,XX,-2,+3,+9,+22	48,XX,-2,+3,+9,+22	48,XX,-2,+3,+9,+22
76	5BA	46,XY,+3,+4,-18,-21	46,XY,+3,+4,-18,-21	46,XY,+3,+4,-18,-21
77	5CB	47,XY,+16,del(20)(q13.2q13.33)	47,XY,+16,del(20)(q13.2q13.33)	47,XY,-1*,+16,-20*,del(5)(q23.1q35.3)*
78	4AB	46,XY,del(6)(q16.1q27)	46,XY,del(6)(q16.1q27)	46,XY,del(6)(q16.1q27)*
79	4BC	46,XX,del(1)(q43q44)	46,XX,del(1)(q43q44)	46,XX,del(1)(q43q44)

Clinical TE-ICM Aneuploid-Aneuploid Imperfect Concordant

Blastocyst Study id#	Gardner Grade	Clinical TE Biopsy	ICM Biopsy	Second TE Biopsy
80	4AC	45,XX,-14	45,XX,-14,del(1)(p36.32p36.12)*	45,XX,-14
81	4BB	45,XY,-16	45,XY,-16,dup(2)(p25.3p23.1)*	45,XY,-16
82	4AA	45,XY,-18	45,XY,-18,dup(2)(q23.3q37.3)*	45,XY,-18
83	5BA	45,XY,-21	45,XY,-21,dup(18)(p11.32q12.1)*	45,XY,-21
84	3BC	45,XX,-22	45,XX,-15*,-22	45,XX,-22
85	4BC	45,X	45,X,+20*,+21*	45,X,+2*,+14*
86	4BB	47,XX,+16	47,XX,+16,dup(5)(q12.1q35.1)*	47,XX,+16
87	5BB	47,XY,+20	47,XY,+20,del(1)(p36.33p33)*	47,XY,+20
88	5CC	46,XX,-10,+15	48,XX,-10*,+15,+17	46,XX,-10,+15
89	4BC	44,XX,-15,-22	44,XX,-15,+18*,-22,dup(1)(q12q44)*	44,XX,-15,-22
90	5BB	44,XY,-21,-22	44,XY,-21,-22,del(1)(p36.33p33)*	44,XY,-21,-22
91	5BC	47,XX,+4,+9,-13	47,XX,+3*,+4,+7*,+9,-13	47,XX,+3*,+4,+7*,+9,-13
92	5CC	47,XX,+20,del(2)(p25.3p24.1)	47,XX,+20,del(2)(p25.3p24.1)*	47,XX,+20,del(2)(p25.3p24.1)
93	5BB	46,XX,del(16)(p13.3p11.2)	45 XX,-16	46,XX,del(16)(p13.3p11.2),dup(16)(p11.2p24.3)*

Clinical TE-ICM Aneuploid-Mosaic Discordant

Blastocyst Study id#		Clinical TE Biopsy	ICM Biopsy	Second TE Biopsy
94	4BC	45,XY,-19	46,XY,-19*	45,XY,-19
95	5AB	47,XY,+6	46,XY,del(4)(q32.1q35.2)*	46,XY

Clinical TE-ICM Aneuploid-Euploid Discordant

Blastocyst Study id#		Clinical TE Biopsy	ICM Biopsy	Second TE Biopsy
96	4AB	47,XX,+12	46,XX	46,XX
97	4BB	46,XX,del(2)(q22.1q31.1)	46,XX	46,XX,del(2)(q22.1q31.1)
98	4BB	46,XY,dup(3)(q26.2q29)(x2)	46,XY	46,XY,dup(3)(q26.2q29)*,dup(22)(q11.1q13.31)*
99	4AB	46,XX,del(9)(q12q34.3)	46,XX	46,XX,del(9)(q12q34.3)*
100	3BB	46,XX,dup(11)(q23.2q25)	46,XX	n/a

*** MOSAIC**

A

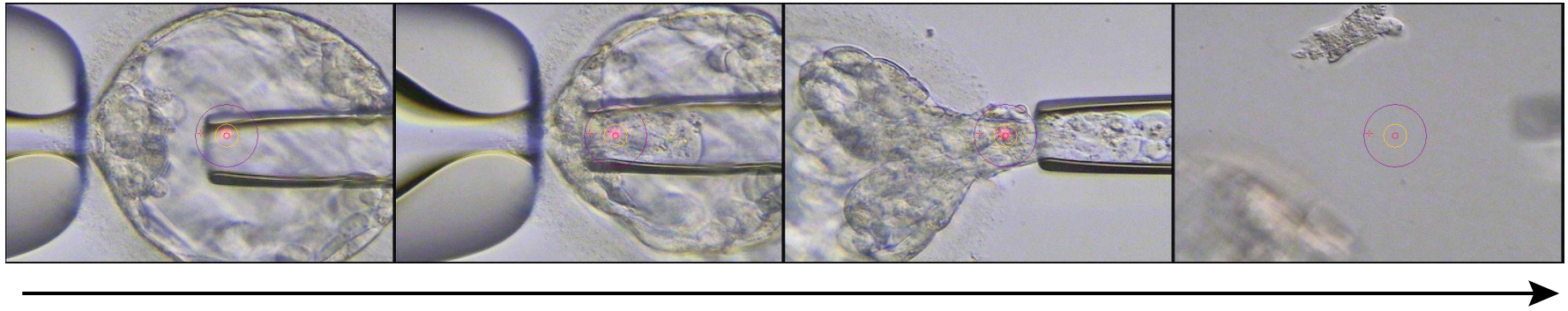

B

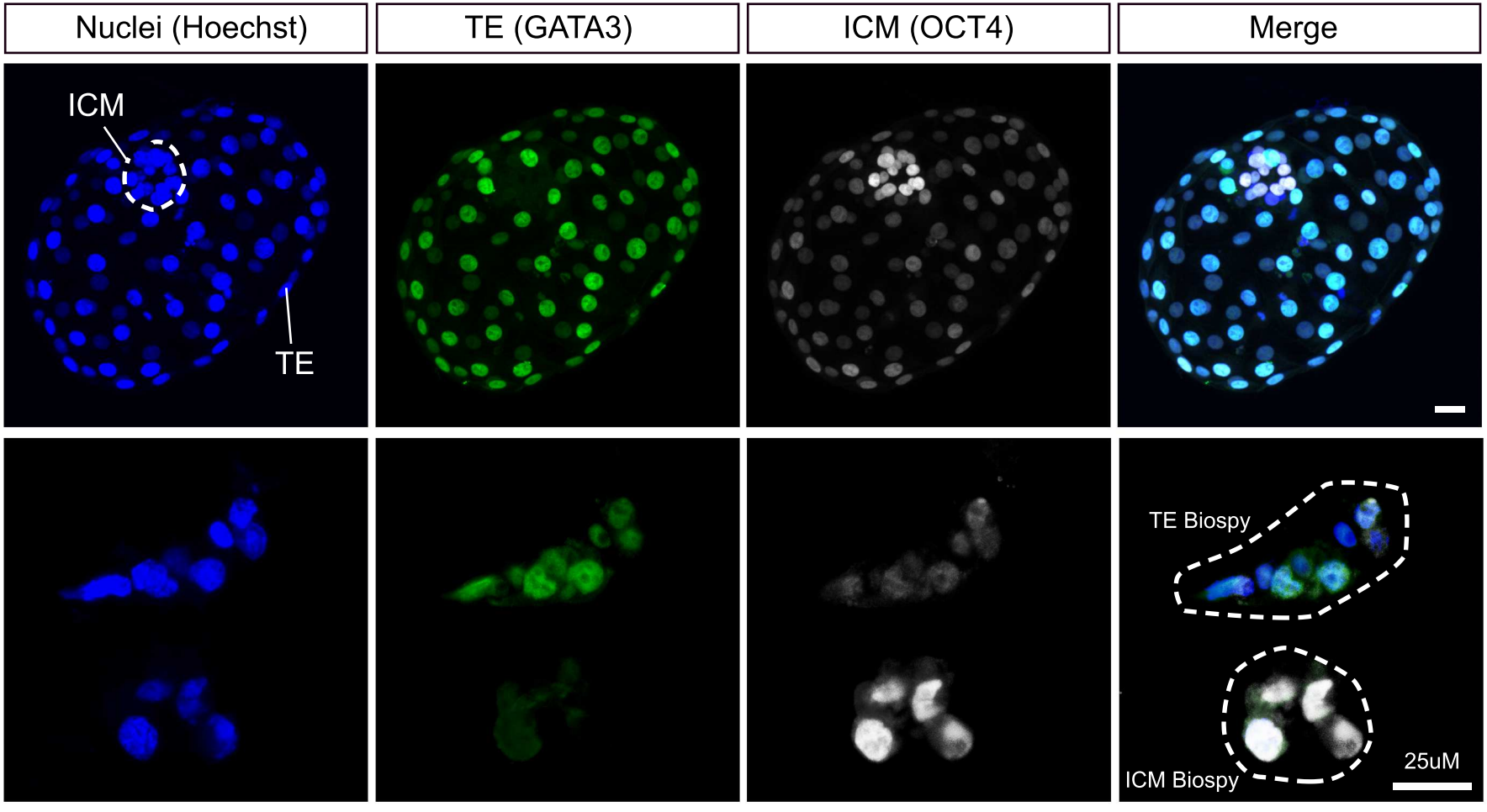
Nuclei (Hoechst)
TE (GATA3)
ICM (OCT4)
Merge
ICM
TE
TE Biospy
ICM Biospy
25uM

FIG1

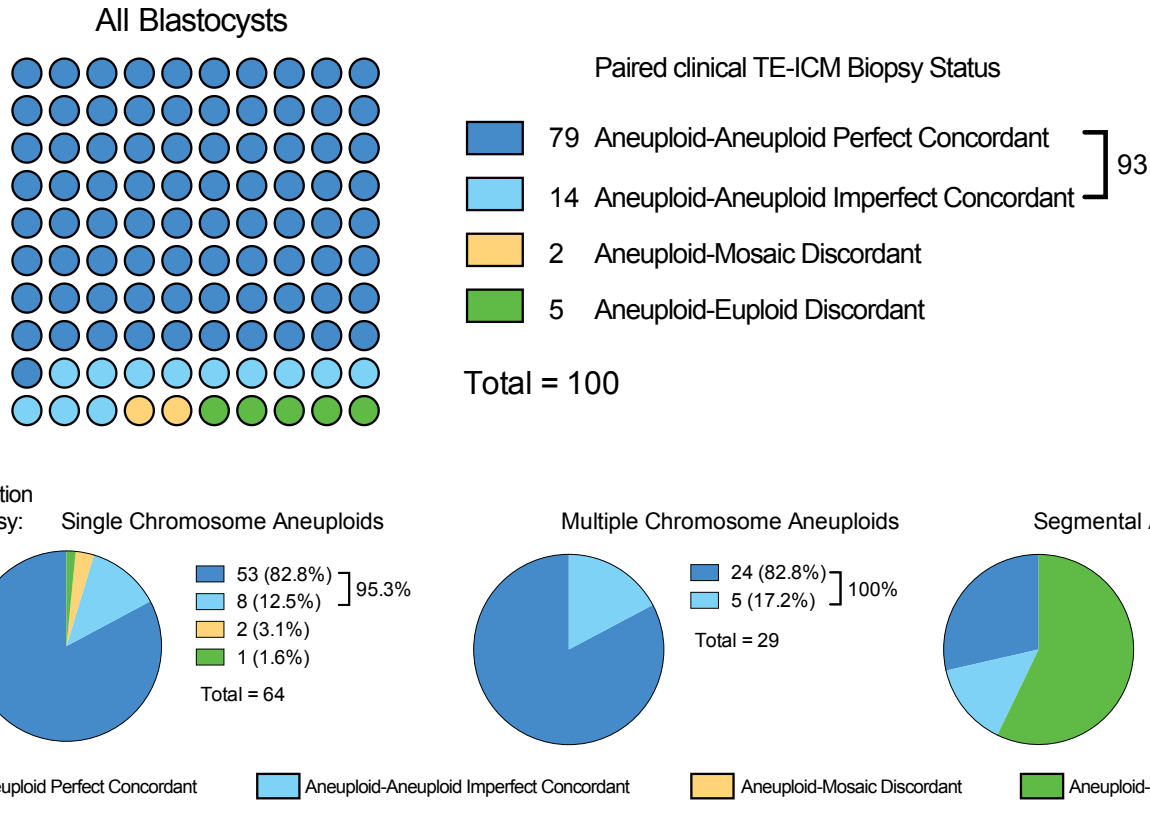
All Blastocysts
Paired clinical TE-ICM Biopsy Status
79 Aneuploid-Aneuploid Perfect Concordant
14 Aneuploid-Aneuploid Imperfect Concordant
93
2 Aneuploid-Mosaic Discordant
5 Aneuploid-Euploid Discordant
Total = 100
Originial Classification by clinical TE biopsy:
Single Chromosome Aneuploids
Paired clin.TE-ICM : Status
53 (82.8%)
8 (12.5%)
95.3%
2 (3.1%)
1 (1.6%)
Total = 64
Multiple Chromosome Aneuploids
24 (82.8%)
5 (17.2%)
100%
Total = 29
Segmental Aneuploids
2 (28.6%)
1 (14.3%)
42.9%
4 (57.1%)
Total = 7
Aneuploid-Aneuploid Perfect Concordant
Aneuploid-Aneuploid Imperfect Concordant
Aneuploid-Mosaic Discordant
Aneuploid-Euploid Discordant

FIG2

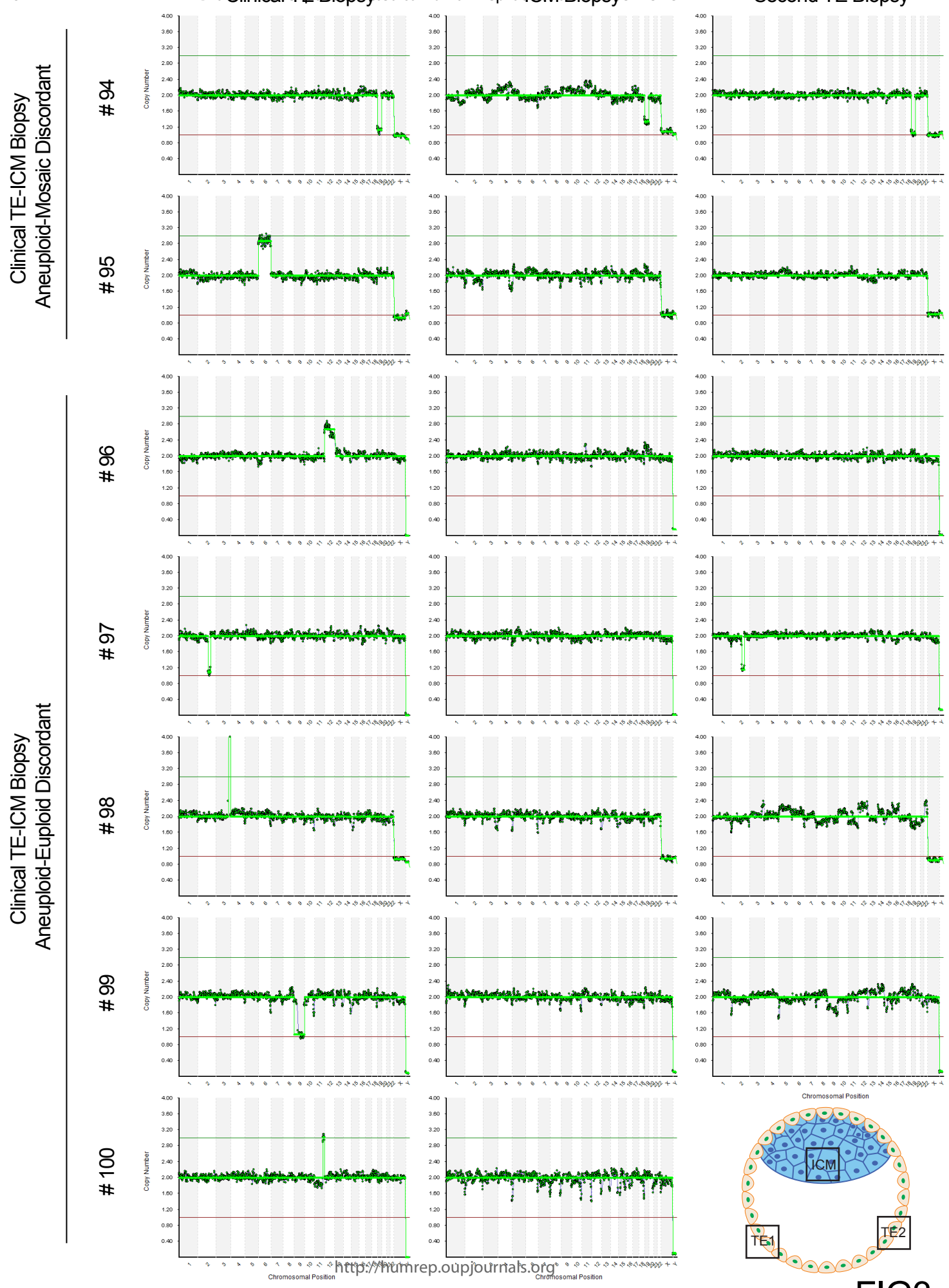
Clinical TE Biopsy
ICM Biopsy
Second TE Biopsy
Clinical TE-ICM Biopsy
Aneuploid-Mosaic Discordant
Clinical TE-ICM Biopsy
Aneuploid-Euploid Discordant
94
95
96
97
98
99
100
Copy Number
Chromosomal Position
ICM
TE1
TE2

FIG3

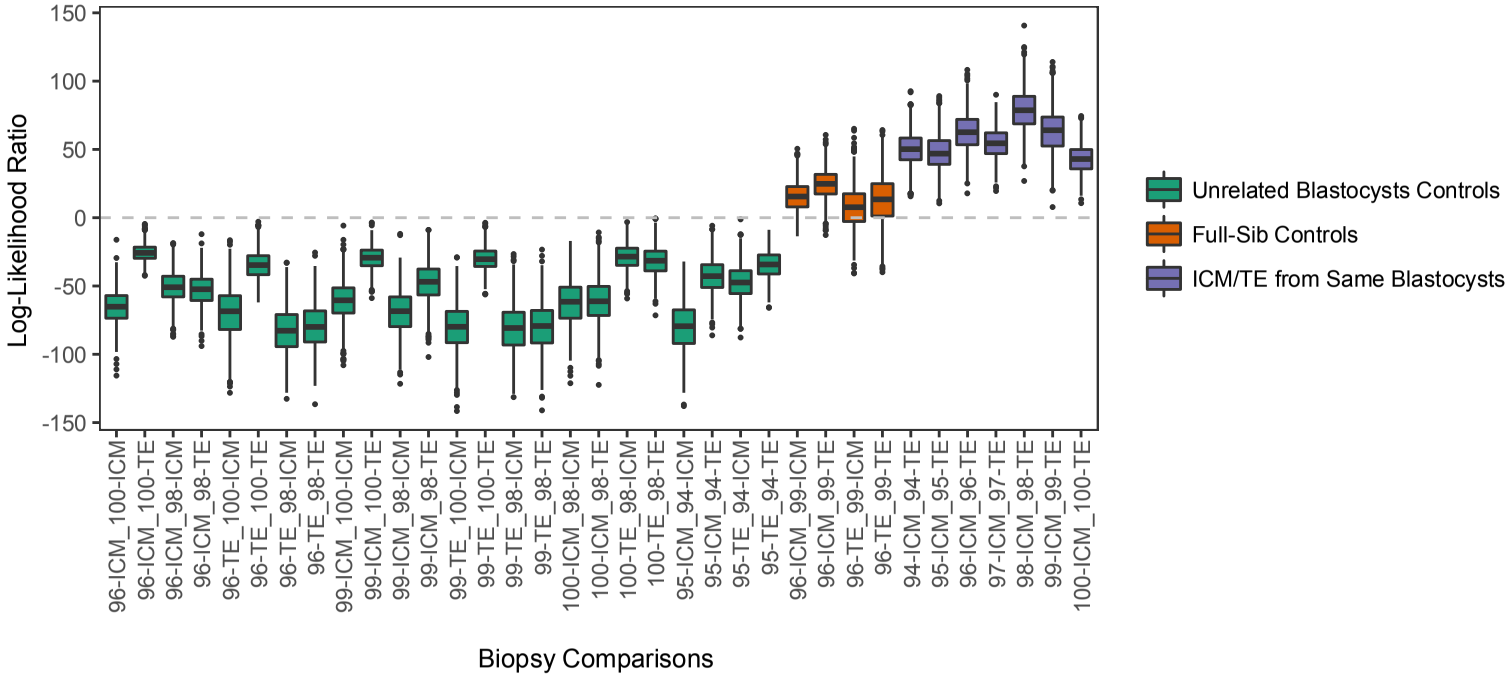
Log-Likelihood Ratio
150
100
50
0
-50
-100
-150
96-ICM_100-ICM
96-ICM_100-TE
96-ICM_98-ICM
96-ICM_98-TE
96-TE_100-ICM
96-TE_100-TE
96-TE_98-ICM
96-TE_98-TE
99-ICM_100-ICM
99-ICM_100-TE
99-ICM_98-ICM
99-ICM_98-TE
99-TE_100-ICM
99-TE_100-TE
99-TE_98-ICM
99-TE_98-TE
100-ICM_98-ICM
100-ICM_98-TE
100-TE_98-ICM
100-TE_98-TE
95-ICM_94-ICM
95-ICM_94-TE
95-TE_94-ICM
95-TE_94-TE
96-ICM_99-ICM
96-ICM_99-TE
96-TE_99-ICM
96-TE_99-TE
94-ICM_94-TE
95-ICM_95-TE
96-ICM_96-TE
97-ICM_97-TE
98-ICM_98-TE
99-ICM_99-TE
100-ICM_100-TE
Biopsy Comparisons
Unrelated Blastocysts Controls
Full-Sib Controls
ICM/TE from Same Blastocysts

FIG4

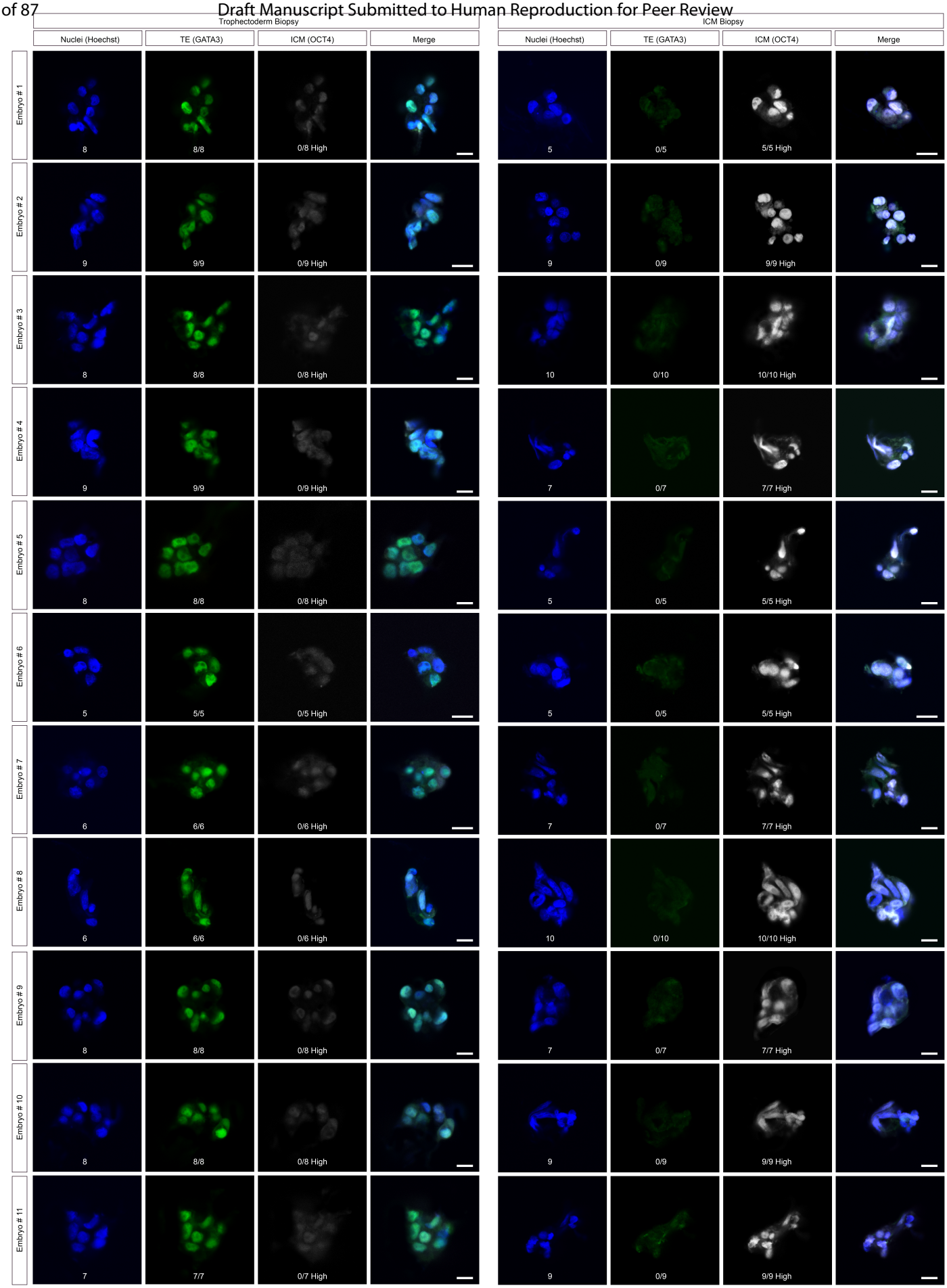

Supplemental FIG1

Supplemental FIG2

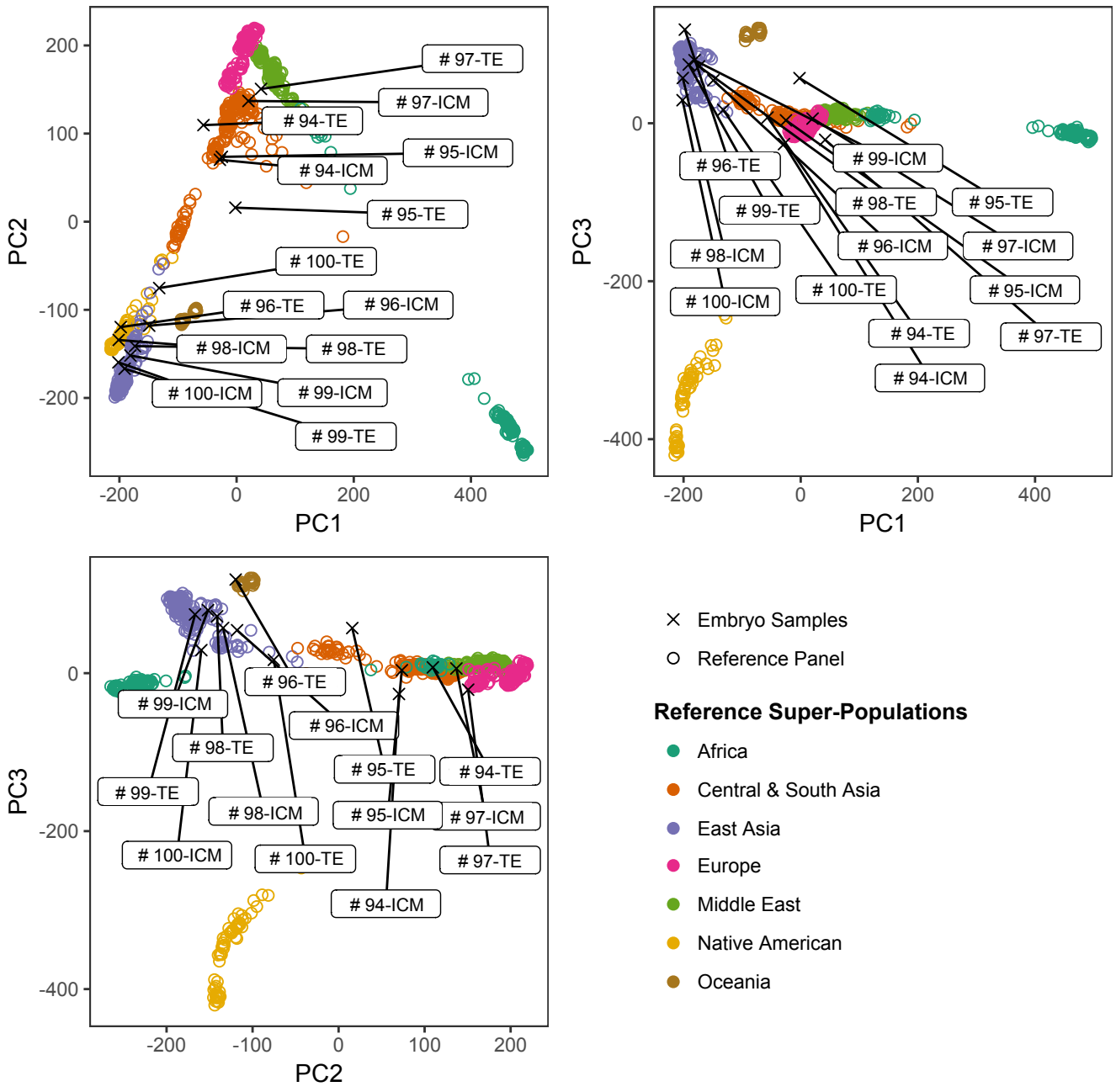

Supplemental FIG3

Blastocyst Stage

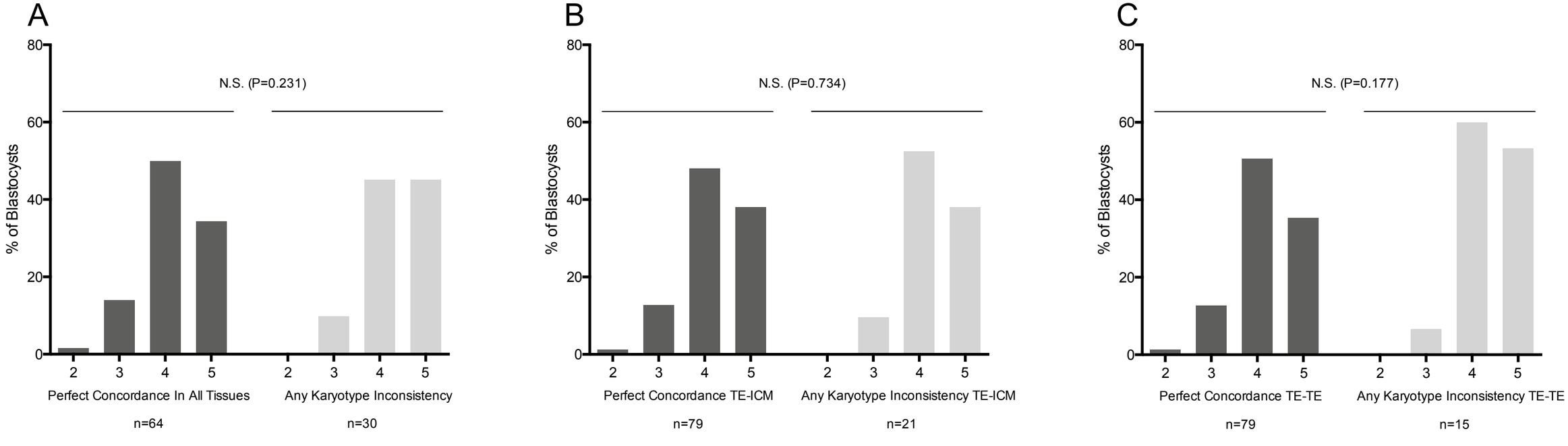

Grade

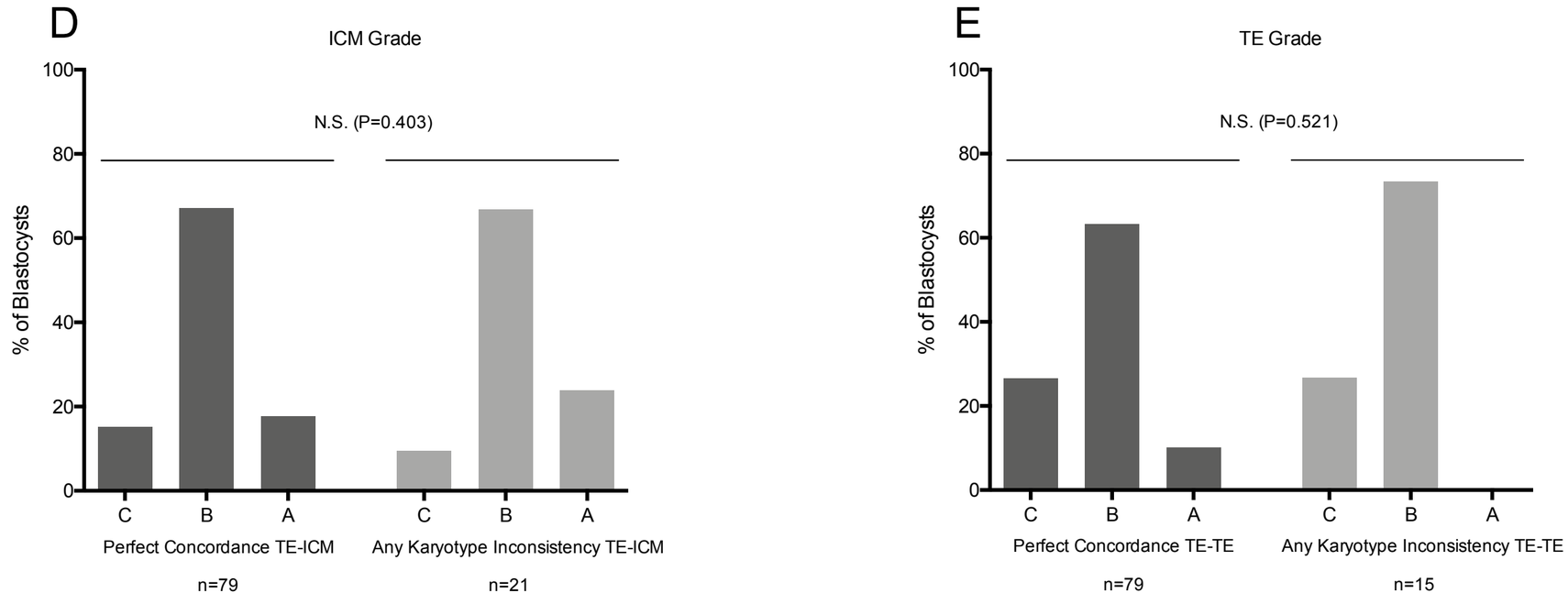

Supplemental FIG. 4

Supplemental Table I.

Blastocyst ID	Primary Ancestry Composition of K = 10 Nearest Neighbors		1000 Genomes Reference Panel Super-Population
	ICM	TE	
#94	C/S Asia	C/S Asia	SAS
#95	C/S Asia	C/S Asia	SAS
#96	East Asia	East Asia	EAS
#97	Europe	Middle East	EUR
#98	East Asia	East Asia	EAS
#99	East Asia	East Asia	EAS
#100	East Asia	East Asia	EAS

Supplemental Data 1

Analysis of tissue relatedness

'Tilde' (Vohr et al., 2015) was used to rule out sample cross-contamination or mislabeling and infer, based on low-coverage sequencing data, whether ICM and TE biopsies were derived from the same blastocyst. This method facilitates indirect comparison of low-coverage samples based on the principle that sparse observed genotypes are informative of genotypes at nearby unobserved markers due to patterns of linkage disequilibrium (LD) in the population.

Reads were mapped to the hg19 reference using the BWA (version 0.7.17) backtrack algorithm with default parameters (Li and Durbin, 2009). We then used the LASER method (version 2.04; (Wang et al., 2015)) to select the appropriate ethnically matched 1000 Genomes Project super-population (Genomes Project et al., 2015) for each blastocyst, as required by tilde. LASER combines genotype imputation with principal components analysis to infer individual ancestry based on low-coverage sequence data. Blastocyst genotypes were visualized in reference ancestry space defined by principal components analysis of the HGDP reference panel (Supplemental Fig. 4; (Li et al., 2008)). Blastocysts were then assigned to corresponding 1000 Genomes super-populations based on ancestries of the K=10 nearest neighbor reference samples in principal components space (Supplemental Table I). In the case of

blastocyst #97, whose ICM and TE biopsies were assigned to European and Middle Eastern reference populations, respectively, we selected the European super-population as the reference panel. We note that these populations fall close to one another in space defined by the top three principal components. Furthermore, Vohr et al. (2015) demonstrated that tilde is relatively robust to misspecification of the reference panel.

Tilde computes a log-likelihood ratio comparing a model in which two samples are derived from the same individual (i.e., same embryo) to a model in which two samples are derived from unrelated individuals (i.e., different embryos). Positive log-likelihood ratios indicate that the data support the former model, while negative log-likelihood ratios indicate that the data support the latter model. Bootstrapping was performed to generate distributions and assess uncertainty in log-likelihood ratio estimates.

As controls, we applied this method to twenty-four comparisons of presumed unrelated embryos as well as four comparisons of full sibling (full-sib) embryos obtained from the same patient. Results from the unrelated negative controls supported the capacity of tilde to distinguish these samples, reflected by negative distributions of log-likelihood ratios (Fig. 4). For all seven embryos producing discordant TE-ICM results, the data supported a model in which the samples were derived from the same corresponding embryo, reflected by positive distributions of log-likelihood ratios. Meanwhile, the full-sib samples from the same patient also produced positive distributions of log-likelihood ratios, but intermediate between the unrelated and same-embryo comparisons, supporting

the power of tilde to distinguish varying levels of relatedness. Together, our data suggest no evidence of cross-contamination or sample mislabeling and substantiate the conclusion that the TE and ICM biopsies of discordant karyotype were derived from the same respective embryos. More generally, our analysis demonstrates that methods such as tilde, which take advantage of patterns of LD in the population, can be useful for research on low-coverage sequencing-based PGT-A datasets.

Supplemental Data 1 Bibliography

Genomes Project, C., Auton, A., Brooks, L.D., Durbin, R.M., Garrison, E.P., Kang, H.M., Korbel, J.O., Marchini, J.L., McCarthy, S., McVean, G.A.*, et al.* (2015). A global reference for human genetic variation. Nature *526*, 68-74.

Li, H., and Durbin, R. (2009). Fast and accurate short read alignment with Burrows-Wheeler transform. Bioinformatics *25*, 1754-1760.

Li, J.Z., Absher, D.M., Tang, H., Southwick, A.M., Casto, A.M., Ramachandran, S., Cann, H.M., Barsh, G.S., Feldman, M., Cavalli-Sforza, L.L.*, et al.* (2008). Worldwide human relationships inferred from genome-wide patterns of variation. Science *319*, 1100-1104.

Vohr, S.H., Buen Abad Najar, C.F., Shapiro, B., and Green, R.E. (2015). A method for positive forensic identification of samples from extremely low-coverage sequence data. BMC Genomics *16*, 1034.

Wang, C., Zhan, X., Liang, L., Abecasis, G.R., and Lin, X. (2015). Improved ancestry estimation for both genotyping and sequencing data using projection procrustes analysis and genotype imputation. Am J Hum Genet *96*, 926-937.